J. Fluid Mech. (2008), vol. 612, pp. 143–152.
doi:10.1017/S0022112008003157 Printed in the United Kingdom

Vortex motion in doubly connected domains

L. ZANNETTI, F. GALLIZIO AND G. M. OTTINO

DIASP, Politecnico di Torino, Corso Duca degli Abruzzi 24, 10129 Torino, Italy

(Received 28 March 2008 and in revised form 11 July 2008)

The unsteady two-dimensional rotational flow past doubly connected domains is analytically addressed. By concentrating the vorticity in point vortices, the flow is modelled as a potential flow with point singularities. The dependence of the complex potential on time is defined according to the Kelvin theorem. The general case of non-null circulations around the solid bodies is discussed. Vortex shedding and time evolution of the circulation past a two-element airfoil and past a two-bladed Darrieus turbine are presented as physically coherent examples.

1. Introduction

The study of the two-dimensional rotational flow in domains confined by multiple bodies is relevant in several problems such as, among many others, the aerodynamics of multiple airfoils, the unsteady motion past multi-bladed vertical-axis wind turbines and the sea motion past islands.

Neglecting the diffusion effects, the flow can be assumed as inviscid and governed by the Euler equations. By concentrating the vorticity on singular vortex particles, the flow reduces to a potential flow affected by vortex singularities. The theory of such a kind of flow is very well established, with the main reference ascribable to Lin (1941), where the Hamiltonian theory of vortex motion in multiply connected domains has in general been set.

Johnson & McDonald (2004) have provided a practical example of such a flow model by studying the interaction of vortices with islands in sea motion. They considered the Hamiltonian motion of a vortex in the doubly connected domain bounded by two circular cylinders, assumed as simple models for islands in the sea. Crowdy & Marshall (2005) generalized the study to any finite number of circular islands. Further examples of vortex motion, in doubly connected domains, have been presented by Johnson & McDonald (2005), who considered the motion of vortices near barrier gaps.

For an inviscid flow with given far-field boundary conditions, the circulations past solid bodies are free parameters which define multiple-flow solutions. In general, physical considerations can help in assuming their values. For instance, in the above-cited works, the circulations around the islands are assumed as null and, on the basis of Kelvin's theorem, kept constant in time. Nevertheless, such an assumption shares the same arbitrariness as any other assumed initial circulation.

In the inviscid framework, vortex-shedding phenomena can reasonably be described when the considered bodies present sharp edges which force the flow to separate. When using a vortex method, the wake issued by the edges can be simulated by adding point vortices which satisfy the Kutta condition at prescribed time intervals. In such a way, the evolution in time of the circulation past each body is defined by the amount of shed vorticity.

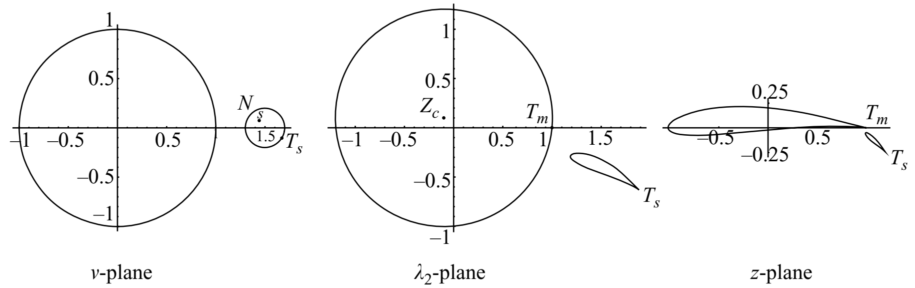

FIGURE 1. $\nu \rightarrow \lambda_2 \rightarrow z$ mapping.

In this work, the motion of vortices in doubly connected domains is addressed for the general case of non-null circulations around bodies. It is shown how the Kelvin theorem defines the time dependence of the complex potential of the motion. Vortex-shedding phenomena in doubly connected domains are described as physically meaningful examples. They are pertinent to the transient fluid motion past a two-element airfoil and past a two-bladed vertical axis wind turbine (VAWT).

2. Flow past a two-element airfoil

The solution of the potential flow past a two-element airfoil has long been known. Lagally (1929) provided the solution of the flow past two circular cylinders and Ferrari (1930) gave the solution for the flow past a biplane section.

First, we recall the steady-flow solution. As shown by Ives (1976), a general mixed analytical–numerical conformal mapping method can be adopted to transform any arbitrary double airfoil section into two circles. For the present purpose of providing an example, the mapping sequence suggested by Ives (1976) is reversed to avoid the numerical part of the transformation and to speed up the flow computation. Instead of mapping a given couple of airfoils in two circles, we transform, in closed form, two given circles into two airfoils. As shown in figure 1, two circles of the complex ν-plane are mapped onto a wing-flap section of the complex z-plane. The main airfoil results in a Kármán–Trefftz airfoil and the flap in a variation of a Kármán–Trefftz airfoil.

On the complex ν-plane, let us consider the (main) unit circle and the (secondary) circle centred at $(x_s, 0)$ and with a radius r_s. The function

$$\frac{\lambda - \lambda_T}{\lambda - \lambda_N}\frac{\lambda - 1/\lambda_T^\star}{\lambda - 1/\lambda_N^\star} = \left(\frac{\nu - \nu_T}{\nu - \nu_N}\frac{\nu - 1/\nu_T^\star}{\nu - 1/\nu_N^\star}\right)^{\tau_s}, \tag{2.1}$$

maps the principal circle onto the unit circle and the secondary circle onto a kind of airfoil of the λ-plane. In (2.1), * denotes complex conjugation, ν_T is located on the circle and corresponds to the trailing edge, ν_N is inside the circle and $\tau_s = 2 - \epsilon_s/\pi$, with ϵ_s being the trailing-edge angle. The final shape of the secondary airfoil depends on the choice of $x_s, r_s, \nu_T, \nu_N, \epsilon_s$. The other parameters λ_T, λ_N, are determined by regularity conditions of the mapping. Details on their determination are given in Ives (1976).

By setting $\lambda_1 = \lambda e^{i\beta}$, the unit circle is rotated by β and, through the further transformation $\lambda_2 = \lambda_1(1 - z_c) + z_c$, it is mapped onto a circle that is centred in z_c and which goes through point $\lambda_2 = 1$. Finally, the Kármán–Trefftz mapping

$$\frac{z-1}{z+1} = \left(\frac{\lambda_2 - 1}{\lambda_2 + 1}\right)^{\tau_m} \tag{2.2}$$

generates the main airfoil and the final shape of the secondary airfoil in the physical

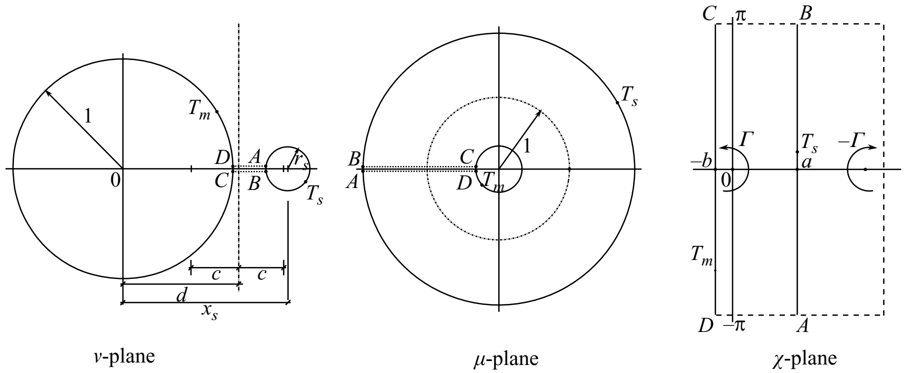

FIGURE 2. $\nu \rightarrow \mu \rightarrow \chi$ mapping.

z-plane. The choice of z_c defines the camber and thickness of the main airfoil and τ_m is $\tau_m = 2 - \epsilon_m/\pi$, with ϵ_m being the trailing-edge angle.

2.1. *The steady flow*

In order to define the flow field, it is convenient to map the region bounded by the airfoils, that is, the region on the outside of the ν-plane circles, inside a rectangle of the complex χ-plane, as shown in figure 2). The two circles of the ν-plane can be considered as belonging to a family of Apollonius circles with foci in $d + c$ and $d - c$, with $d = (x_s^2 - r_s^2 + 1)/2x_s$ and $c = \sqrt{(x_s - d)^2 - r_s^2}$. The mapping $\nu_1 = (\nu - d)/c$ brings the foci into $\nu_1 = \pm 1$ and the transformation $\mu = (\nu_1 + 1)/(\nu_1 - 1)$ maps the region bounded by the two circles on an annulus of the μ-plane, whose outer boundary is a circle with radius $\rho_s > 1$, which corresponds to the secondary airfoil, and whose inner boundary is a circle with radius $\rho_m < 1$, corresponding to the main airfoil. Finally, $\chi = \log(\mu)$ maps the annulus in the rectangle $-b \leqslant \mathrm{Re}(\chi) \leqslant a$, $-\pi \leqslant \mathrm{Im}(\chi) \leqslant \pi$, with $b = -\log(\rho_m)$ and $a = \log(\rho_s)$.

Briefly, the chain mapping $\chi \rightarrow z$ is such that the left-hand side of the above-defined rectangle is mapped onto the main airfoil, the right-hand side onto the secondary airfoil and the origin of the χ-plane onto the point at infinity of the z-plane. The upper and lower sides of the rectangles are periodic boundaries that correspond to a single line which connects the two airfoils of the z-plane.

Following the same reasoning as Lagally (1929) and Ferrari (1930), the complex velocity $\mathrm{d}w/\mathrm{d}\chi$ in the χ-plane, with w denoting the complex potential, has to be expressed by a doubly periodic function. The impermeability condition of the solid boundaries can, in fact, be enforced by infinite reflections with respect to the vertical sides of the rectangle and as a consequence, the complex velocity has to be periodic, possessing as semiperiod $\omega = a + b$. Moreover, as a result of the mapping, the velocity has to hold the further imaginary semiperiod $\omega' = \mathrm{i}\pi$.

With reference to figure 2, let the rectangle $-b \leqslant \mathrm{Re}(\chi) \leqslant 2a + b$, $-\mathrm{i}\pi \leqslant \mathrm{Im}(\chi) \leqslant \mathrm{i}\pi$ be assumed as the fundamental rectangle. The regularity of the flow field implies that $\mathrm{d}w/\mathrm{d}\chi$ can have singularities only at $\chi = 0$, $\chi = 2a$. These can be second-order poles and first-order poles which represent, at the infinity of the physical z-plane, a non-null flow velocity and a vortex, respectively. According to the above-stated double periodicity, $\mathrm{d}w/\mathrm{d}\chi$ is then expressed by the elliptic function:

$$\frac{\mathrm{d}w}{\mathrm{d}\chi} = -[Q^{\star}_{\infty}\wp(\chi) - Q_{\infty}\wp(\chi - 2a)] + \frac{\Gamma}{2\pi \mathrm{i}}[\zeta(\chi) - \zeta(\chi - 2a)] + \mathrm{i}\kappa, \qquad (2.3)$$

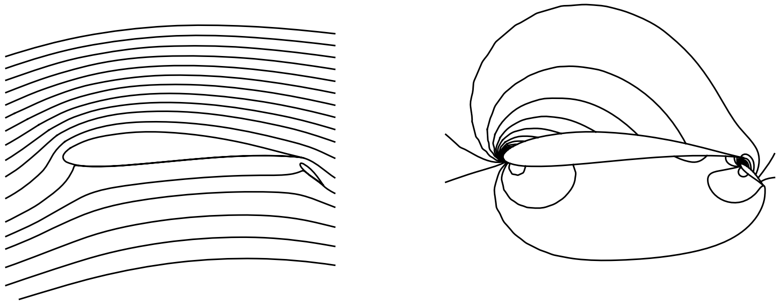

FIGURE 3. Streamline and C_p patterns for the steady flow at $\alpha = 5°$.

where ζ and $\wp$ are the Weierstrass functions that express the first- and second-order poles, respectively, and κ is a real constant. By integration, the complex potential then becomes

$$w = Q_\infty^\star \zeta(\chi) - Q_\infty \zeta(\chi - 2a) + \frac{\Gamma}{2\pi i} \log \frac{\sigma(\chi)}{\sigma(\chi - 2a)} + i\kappa\chi, \tag{2.4}$$

where the Weierstrass σ function has been introduced.

The value of the parameter $Q_\infty^\star$ is defined by the complex velocity at infinity in the physical plane $q_\infty^\star = \lim_{\chi \to 0}(dw/d\chi)/(dz/d\chi)$, which yields

$$Q_\infty^\star = -2q_\infty^\star \frac{c(1 - z_c)e^{-i\beta}}{\tau_s\, \tau_m} \frac{\lambda_T - \lambda_N + 1/\lambda_T^\star - 1/\lambda_N^\star}{\nu_T - \nu_N + 1/\nu_T^\star - 1/\nu_N^\star}.$$

According to the theory, two elliptic functions with the same poles can only differ for a constant, and thus (2.3) is unique once κ is defined. The Kutta condition, that is, $(dw/d\chi)_{\chi_{T_m}, \chi_{T_s}} = 0$, establishes the values of Γ and κ, with χ_{T_m}, χ_{T_s} being the images of the trailing edges on the χ-plane.

Let γ_m, γ_s denote the circulations past the main and secondary airfoils, respectively, then $\Gamma = -(\gamma_m + \gamma_s)$, that is, Γ is the opposite of the total circulation past the two airfoils. With reference to figure 2, $\gamma_m = w_C - w_D$, that is, by exploiting the quasi-periodicity properties of the ζ and σ functions (see Tricomi 1951),

$$\gamma_m = -4i\eta' \left[\mathrm{Im}(Q_\infty) + \frac{\Gamma a}{2\pi} \right] - 2\pi\kappa, \qquad \gamma_s = -\Gamma - \gamma_m, \tag{2.5}$$

with $\eta' = \zeta(\omega')$.

An example of a flow past a double airfoil is represented in figure 3 where the streamline and C_p patterns are pertinent to an airfoil at angle of incidence $\alpha = 5°$.

2.2. *Transient flow*

In order to represent a physically meaningful unsteady rotational flow field, let us consider the transient that follows the impulsive starting of the above double airfoil.

At the initial time, the flow is at rest and the total circulation is null. Once the flow is started, vorticity is shed into the wakes. According to a discrete vortex method (see, for instance, Clements 1973), the wake can be modelled by concentrating the vorticity in point vortices. According to such a model, at fixed time steps, a point vortex is added to each airfoil in a fixed location close to the trailing edge, with a γ_j circulation defined by the Kutta condition. As the added vortices move, the Kutta condition is violated, but it is restored as soon as another two vortices are released.

This discrete approximation of the continuous evolution of smooth trailing-edge vortex sheets has been discussed in the literature (see, for instance, Clements 1973;

Sarpkaya 1975; Kiya & Arie 1977 and references therein). A heuristic choice of parameters, as release timing and location, is required. This choice has a negligible effect on a possible asymptotic steady solution, but it affects the accuracy of the description of a transient flow. The vortex method here used is the same as in Zannetti & Iollo (2003), where the choice of the parameters was based on the thumb rules suggested in literature and on numerical experiments. A sort of validation has been obtained by checking the ability of the method to predict the correct Strouhal numbers of flat plates at incidence and to provide the self-similar structure of rolled-up vortex-sheets (see Pullin 1978). Assuming q_∞ as the reference velocity and $c/2$ as the reference length, with c being the main airfoil chord, the release locations have been set downstream from the trailing edges at the distance $d=0.01$, which is in the range of the values recommended in literature. With a second-order integration time step $dt=0.001$, the release interval has been set at $dt_r=k\,dt$, with k varying from $k=1$, for short time transients, to $k=10$, for longer simulations.

Following the above reasoning concerning the steady flow, the χ-plane complex velocity and complex potential are

$$\frac{\mathrm{d}w}{\mathrm{d}\chi}=-[Q_\infty^\star\wp(\chi)-Q_\infty\wp(\chi-2a)]+\frac{1}{2\pi\mathrm{i}}\sum_{j_m=1}^{N}\gamma_{j_m}[\zeta(\chi-\chi_{j_m})-\zeta(\chi+\chi_{j_m}^\star-2a)]$$
$$+\frac{1}{2\pi\mathrm{i}}\sum_{j_s=1}^{N}\gamma_{j_s}[\zeta(\chi-\chi_{j_s})-\zeta(\chi+\chi_{j_s}^\star-2a)]+\mathrm{i}\kappa(t),\quad(2.6)$$

$$w=Q_\infty^\star\zeta(\chi)-Q_\infty\zeta(\chi-2a)+\frac{1}{2\pi\mathrm{i}}\sum_{j_m=1}^{N}\gamma_{j_m}\log\frac{\sigma(\chi-\chi_{j_m})}{\sigma(\chi+\chi_{j_m}^\star-2a)}$$
$$+\frac{1}{2\pi\mathrm{i}}\sum_{j_s=1}^{N}\gamma_{j_s}\log\frac{\sigma(\chi-\chi_{j_s})}{\sigma(\chi+\chi_{j_s}^\star-2a)}+\mathrm{i}\kappa(t)\chi,\quad(2.7)$$

where the m and s subscripts refer to vortices shed by the main and secondary airfoils, respectively, N is the number of the released vortex couples, $\chi_{j_{m,s}}$ are their locations and $\kappa(t)$ is a real function of time, for now unknown, which uniquely defines the elliptic function (2.6).

According to the Kelvin theorem, during the transient, the sum of the bound circulation and shed circulation has to be null for each airfoil, that is, $\gamma_m=-\sum\gamma_{j_m}$, $\gamma_s=-\sum\gamma_{j_s}$. With reference to figure 2, by definition

$$\mathrm{Re}\oint\frac{\mathrm{d}w}{\mathrm{d}\chi}\mathrm{d}\chi=-(w_C-w_D)-(w_A-w_B)=\sum_{j_m=1,\,j_s=1}^{N}(\gamma_{j_m}+\gamma_{j_s})$$

and

$$(w_C-w_D)=\gamma_m,\qquad(w_A-w_B)=\gamma_s;$$

it follows that function $\kappa(t)$ is established by enforcing either

$$(w_C-w_D)=-\sum_{j_m}^{N}\gamma_{j_m}\quad\text{or}\quad(w_A-w_B)=-\sum_{j_s}^{N}\gamma_{j_s}.\qquad(2.8a,b)$$

For this purpose, in order to manage easily the branch cuts which connect points $(\chi_{j_{m,s}})$ and $(2a-\chi_{j_{m,s}}^\star)$, it is convenient to use (2.8a), which yields

$$\kappa=\frac{1}{2\pi}\left\{\sum_{j_m=1}^{N}\gamma_{j_m}+2\frac{\eta'}{\mathrm{i}\,\pi}\sum_{j_{m,s}=1}^{2N}\gamma_{j_{m,s}}[a-\mathrm{Re}(\chi_{j_{m,s}})]-4\mathrm{i}\,\eta'\mathrm{Im}(Q_\infty)\right\},\qquad(2.9)$$

which has been obtained by using the quasi-periodicity properties of the Weierstrass ζ and σ functions.

Equation (2.9) defines function $\kappa(t)$ through the dependence, on time, of the vortex locations $\chi_{j_{m,s}}(t)$ during their motion.

Moreover, each time two new vortices are shed, the Kutta condition is enforced, that is, the two equations $(\mathrm{d}w/\mathrm{d}\chi)_{\chi_{T_m}} = (\mathrm{d}w/\mathrm{d}\chi)_{\chi_{T_s}} = 0$ are set. Together with (2.9), they form a set of three linear equations for the unknown value of κ and the unknown values of the circulations $\gamma_{N_m}, \gamma_{N_s}$ of the newly arisen vortices.

Johnson & McDonald (2004) considered the case where $q_\infty = 0$, $\gamma_m = \gamma_s = 0$, with no vortex shedding taking place and with N free point vortices in the flow field. Since $(w_C - w_D) + (w_B - w_A) = 0$, the total circulation is null, which implies a vortex at infinity, that is, at $\chi = 0$, whose strength is $\Gamma = -\sum_{j=1}^{N} \gamma_j$. Exploiting the relation between the Weierstrass σ and Jacobi ϑ_1 functions, (2.7) reduces to (2.11) of Johnson & McDonald (2004), plus a negligible constant.

The vortex method implemented here is based on integrating in time the vortex locations on the transformed χ-plane and then on mapping them on the physical z-plane. Let the subscript j denote either j_m or j_s, therefore $\dot{\chi}_j^\star = \dot{z}_j^\star/(\mathrm{d}z/\mathrm{d}\chi)^\star$. According to the Routh (1881) rule (see also Clements 1973; Saffman 1992),

$$\dot{z}_j^\star = \left(\chi_j'^\star - \frac{\gamma_j}{4\pi\mathrm{i}} \frac{\mathrm{d}^2 z/\mathrm{d}\chi^2}{\mathrm{d}z/\mathrm{d}\chi}\right) / (\mathrm{d}z/\mathrm{d}\chi) \text{ hence } \dot{\chi}_j^\star = \left(\chi_j'^\star - \frac{\gamma_j}{4\pi\mathrm{i}} \frac{\mathrm{d}^2 z/\mathrm{d}\chi^2}{\mathrm{d}z/\mathrm{d}\chi}\right) / J, \tag{2.10}$$

where J is the mapping Jacobian $J = |\mathrm{d}z/\mathrm{d}\chi|^2$ and $\chi_j'^\star$ is the velocity that a free vortex should possess through advection on the χ-plane, that is,

$$\begin{aligned}\chi_j'^\star = \lim_{\chi \to \chi_j} \left(\frac{\mathrm{d}w}{\mathrm{d}\chi} - \frac{\gamma_j}{2\pi\mathrm{i}} \frac{1}{\chi - \chi_j}\right) &= -[Q_\infty^\star \wp(\chi_j) - Q_\infty \wp(\chi_j - 2a)] \\ &+ \frac{1}{2\pi\mathrm{i}} \left[\sum_{n=1, n\neq j}^{2N} \gamma_n \zeta(\chi_j - \chi_n) - \sum_{n=1}^{2N} \gamma_n \zeta(\chi_j + \chi_n^\star - 2a)\right] + \mathrm{i}\kappa(t).\end{aligned}$$

The Hamiltonian H, which is pertinent to the vortex motion on the physical z-plane, can be written in parametric form, with χ as the parameter. According to Lin (1941),

$$\begin{aligned}H = &\sum_{i=1}^{2N} \gamma_i \,\mathrm{Im}[Q_\infty^\star \zeta(\chi_i) - Q_\infty \zeta(\chi_i - 2a) + \mathrm{i}\kappa\, \chi_i] - \sum_{i>j, j=1}^{2N} \frac{\gamma_i \gamma_j}{2\pi} \log \left|\frac{\sigma(\chi_i - \chi_j)}{\sigma(\chi_i + \chi_j^\star - 2a)}\right| \\ &+ \sum_{i=1}^{2N} \frac{\gamma_i^2}{4\pi} \log|\sigma(\chi_i + \chi_i^\star - 2a)| + \sum_{i=1}^{2N} \frac{\gamma_i^2}{4\pi} \log\left|\frac{\mathrm{d}z}{\mathrm{d}\chi}\right|.\end{aligned}$$

As in Zannetti & Franzese (1994), the (ξ, η)-coordinates of the χ-plane $(\xi + \mathrm{i}\eta = \chi)$ can be assumed as non-canonical variables, so that the Hamiltonian system governing the vortex motion takes the form

$$\gamma_i \dot{\xi}_i = (\partial_{\eta_i} H)/J, \qquad \gamma_i \dot{\eta}_i = -(\partial_{\xi_i} H)/J,$$

which is equivalent to (2.10).

A simulation of a transient flow has been computed for the same flow whose asymptotic steady state was computed above. Figure 4, on the lower side, shows two snapshots of the initial rolling up of the wakes released by the trailing edges of the two airfoils. The history, in time, of the circulations around the airfoils is presented on the upper side and it shows how the circulations asymptotically tend to the stationary values.

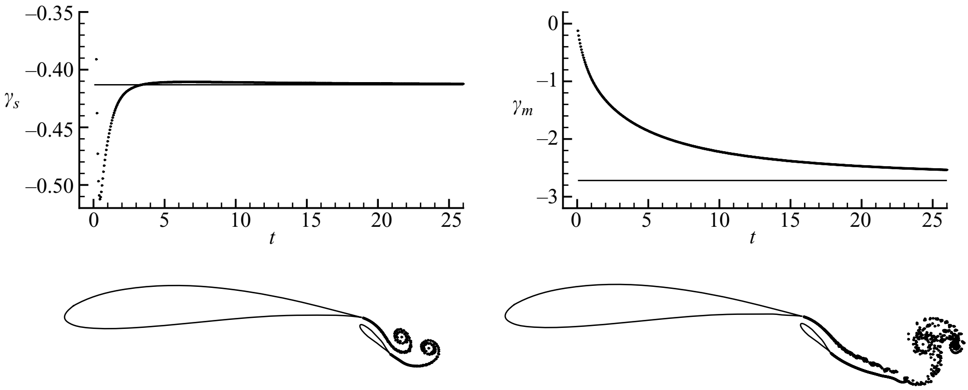

FIGURE 4. Time history of the airfoil circulations and wake snapshots at $t = 0.3$, $t = 0.7$, and with $2N = 600$, $2N = 1400$ vortices, respectively.

3. Two-bladed Darrieus turbine

According to the Riemann mapping theorem, any doubly connected domain can be conformally mapped onto an annulus with a fixed radius ratio. As a consequence, the above investigation is general and the study of any topologically equivalent flow can be based on it.

Although the above example of unsteady flow is somewhat academic, here, as a further example, an application is presented where the unsteadiness is unavoidable and essential, and where the behaviour of unsteady wakes has an important effect on the performances of a fluid dynamic device. Moreover, the unsteady character of the flow analysed here is more general, being relevant to moving bodies.

A two-bladed vertical axis wind turbine (VAWT) with a Darrieus architecture is taken into consideration. It consists of two straight blades rotating around a vertical, that is, orthogonal to the wind shaft. During each cycle, the blades undergo a highly unsteady relative fluid motion with large oscillation of the incidence and, as a consequence, the circulation past them varies in time, and vorticity is shed into the wakes. In addition, the blade trajectories intersect the wakes and affect the turbine performances to a great extent. The description of such an unsteady flow is therefore useful to understand the phenomena and to improve the design of such a VAWT.

Peculiar blade sections, bearing vortex-trapping cavities to prevent the occurrence of dynamic stall, were proposed in Zannetti, Gallizio & Ottino (2007), where the unsteady flow field was described by a vortex method that is similar to the present one, but the above-discussed time dependence of the parameter κ was neglected. In the present work, the complex potential is emended according to the above analysis. For the sake of simplicity, traditional blade sections, without vortex-trapping cavities are considered, as the extension of the present formulation to any more general doubly connected domain is straightforward.

With the same spirit as in the double airfoil analysis, the blade sections are here defined by simple analytic functions, in closed form, starting from circles.

The mapping sequence is shown in figure 5. Let us consider the annulus formed by the circles centred on the origin of the μ-plane and with the radii $L < 1$ and $1/L$, respectively. The bilinear function

$$\nu = \mathrm{i}\,\eta_o \frac{1+\mu}{1-\mu}$$

maps the two circles onto the two mirrored Apollonius circles c_u, c_d of the ν-plane, which have the foci at $\nu_o = \pm\,\mathrm{i}\,\eta_o$, the centres at $\nu_c = \pm\,\nu_o(1+L^2)/(1-L^2)$ and the

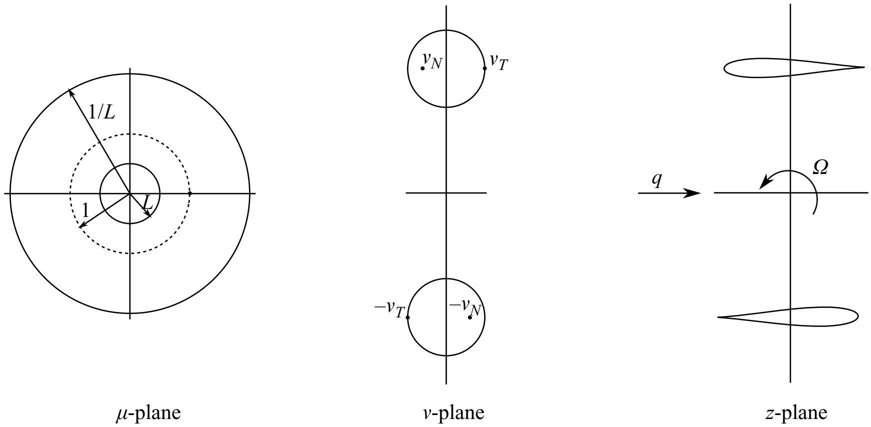

FIGURE 5. VAWT mapping.

same radius $\rho_c = 2\,L\,\eta_o/(1-L^2)$. Finally, the mapping

$$\frac{z^2 - z_T^2}{z^2 - z_N^2} = \left(\frac{\nu^2-\nu_T^2}{\nu^2-\nu_N^2}\right)^{\tau}, \qquad \tau = 2 - \frac{\epsilon}{\pi},$$

generates the two blades on the physical z-plane. This mapping is such that the two blades can be superimposed through a 180° rotation. The blade geometry and turbine aspect ratio are defined by the parameters η, ν_t and ν_n, with $\pm\nu_t$ being relevant to the trailing edges and $\pm\nu_N$ being inside the circles. The values of z_T, z_N are defined by the conditions $z(0)=0$ and $\lim_{\nu\to\infty} \mathrm{d}z/\mathrm{d}\nu = 1$, that is,

$$z_T^2 = \tau\,\nu_T^2 \frac{1-(\nu_N/\nu_T)^2}{1-(\nu_N/\nu_T)^{2\tau}}, \qquad z_N^2 = [z_T(\nu_N/\nu_T)^{\tau}]^2.$$

Let the blades be spinning with the angular velocity Ω around the origin of the z-plane. According to the Milne-Thomson (1968) approach, the complex potential w of the absolute motion is expressed in a frame of reference which moves with the body, that is, the z-plane is considered as rotating around its origin with the turbine angular velocity Ω. According to the absolute nature of the flow motion, the streamfunction is not constant on the blade contours, but has a value that is defined by the condition of impermeability.

The complex potential can be expressed as the sum of two terms, $w = w_1 + w_2$, where w_1 is such that the streamfunction on the blade surfaces will have a constant value and w_2 is such that the streamfunction will assume the values which satisfy the impermeability condition.

Let the μ-plane be mapped onto the χ-plane by $\chi = \log\mu$. As above, the annulus is thus mapped onto a rectangle, with $a = b = -\log(L)$, and the term w_1 can be assumed as coincident with the potential expressed by (2.7), with $Q_\infty = 2\,\mathrm{i}\,\eta_o\,q_\infty \exp(\mathrm{i}\,\alpha)$, and with the subscripts m and s pertinent to the upper and lower blades of figure 5, respectively. It should be noted that the wind velocity direction $\alpha = -\Omega\,t$ depends on time.

The term w_2 should not add any singularity to the flow field and as a consequence, its general expression can be written as a Laurent series which converges inside the annulus of the μ-plane, that is,

$$w_2 = \sum_{n=1}^{\infty}(a_n + \mathrm{i}b_n)(L\mu)^{n-1} + \sum_{n=1}^{\infty}(c_n + \mathrm{i}d_n)(\mu/L)^{-(n-1)}.$$

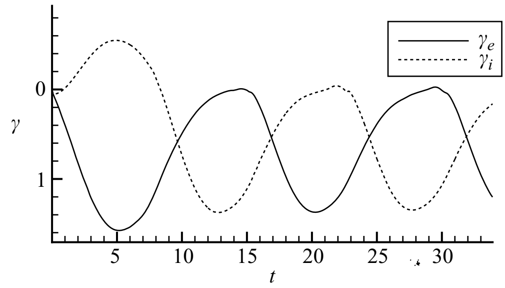

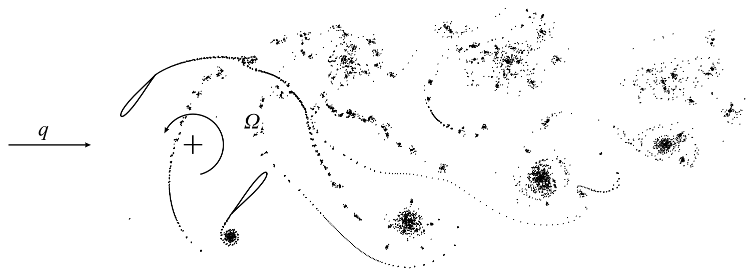

FIGURE 6. Time history of the blade circulations and wake visualization at $t = 28.5$ with $2N = 12\,400$ vortices.

Let $z = z(\mu)$ be the $\mu \rightarrow z$ mapping, with $\mu = \rho \exp(\mathrm{i}\varphi)$, the impermeability condition (Milne-Thomson 1968) yields

$$\psi_s = -\frac{1}{2}\Omega|z(\mathrm{e}^{\mathrm{i}\varphi}/L)|^2, \qquad \psi_m = -\frac{1}{2}\Omega|z(L\mathrm{e}^{\mathrm{i}\varphi})|^2,$$

where the subscripts m and s refer to the interior and exterior circles of the μ-plane annulus, respectively. The following two relationships can hence be derived:

$$\psi_s = \sum_{n=1}^{N}(b_n + d_n L^{2n-2})\cos(n-1)\varphi + (a_n - c_n L^{2n-2})\sin(n-1)\varphi,$$

$$\psi_m = \sum_{n=1}^{N}(b_n L^{2n-2} + d_n)\cos(n-1)\varphi + (a_n L^{2n-2} - c_n)\sin(n-1)\varphi,$$

which allow the coefficients a_n, b_n, c_n, d_n of the above series, suitably truncated, to be evaluated and thus the complex potential w to be fully defined.

In the same way as described for the two-element airfoil, the function $\kappa(t)$ can be defined by satisfying the Kelvin theorem for each blade. Let us assume that, at the initial time, the turbine and the flow are at rest and as a consequence, the total circulation and the circulation around each blade are null. During the motion, the sum of the bound and shed circulations should remain null for each blade. As for the above two-element airfoil, the enforcing of one of (2.8a, b) suffices to satisfy the requirement. Since, on the χ-plane, w_2 is periodic with the period $2\pi\mathrm{i}$, (2.9) determines the function $\kappa(t)$ as above.

The strengths of the shed vortices are determined by enforcing the Kutta condition. For moving bodies, it can be expressed by the requirement that the relative velocity is non-singular at the trailing edges. Let us denote the streamfunction of the relative motion with ψ_r and the angle between the radial r and the normal to the body n directions with δ, therefore

$$\lim_{z \rightarrow z_{T_{m,s}}} \frac{\partial \psi_r}{\partial n} = \lim_{z \rightarrow z_{T_{m,s}}} [\mathrm{Im}(\mathrm{d}w/\mathrm{d}\chi)|\mathrm{d}\chi/\mathrm{d}z| + \Omega|z|\cos\delta] \neq \infty.$$

Since $d\chi/dz \to \infty$ at the trailing edges, the Kutta condition is expressed by the equations $\mathrm{Im}(dw/d\chi)_{T_{m,s}} = 0$.

A snapshot of the wakes issued by the blades and the time history of the bound circulations is presented in figure 6 for a turbine with the chord/radius ratio $c/R = 0.74$ and with the wind/blade-speed ratio $q_\infty/\Omega\, R = 0.88$.

4. Conclusions

A theory of the vortex motion past bodies possessing circulation has been presented for doubly connected domains.

As paradigmatic examples, the inviscid rotational flows, that follow an impulsive start, have been described by a vortex method for an airfoil-flap section and for a two-bladed Darrieus wind turbine.

The flow field has been transformed, by conformal mapping, into a doubly periodic domain where the complex velocity is expressed by an elliptic function, which, according to the theory, is unique once an additive function $\kappa(t)$ is defined. This function is established by the Kelvin theorem, that is, by the physical requirement that the sum of the bound and shed circulations past each body must remain constant.

REFERENCES

Clements, R. R. 1973 An inviscid model of two-dimensional vortex shedding. *J. Fluid Mech.* **57**, 321–336.

Crowdy, D. G. & Marshall, J. S. 2005 The motion of a point vortex around multiple circular islands. *Phys. Fluids* **17**, 56602–13.

Ferrari, C. 1930 Sulla trasformazione conforme di due cerchi in due profili alari. *Mem. R. Acc. Sci. Torino* **68**, 1–15.

Ives, D. C. 1976 A modern look at conformal mapping, including multiply connected regions. *AIAA J.* **14**, 1006–1011.

Johnson, E. R. & McDonald, N. R. 2004 The motion of a vortex near two circular cylinders. *Proc. R. Soc. Lond.* A **460**, 939–954.

Johnson, E. R. & McDonald, N. R. 2005 Vortices near barriers with multiple gaps. *J. Fluid Mech.* **531**, 335–358.

Kiya, M. & Arie, M. 1977 A contribution to an inviscid vortex-shedding model for an inclined flat plate in uniform flow. *J. Fluid Mech.* **82**, 223–243.

Lagally, M. 1929 Die reibungslose stromung im aussengbiet zweier kreise. *Z. Angew. Math. Mech.* **9**, 299–305.

Lin, C. C. 1941 On the motion of vortices in two dimensions. *Proc. Nat. Acad. Sci. USA* **27**, 570–577.

Milne-Thomson, L. M. 1968 *Theoretical Hydrodynamics*. Dover.

Pullin, D. I. 1978 The large-scale structure of unsteady self-similar rolled-up vortex-sheets. *J. Fluid Mech.* **88**, 401–430.

Routh, E. J. 1881 Some application of conjugate functions. *Proc. Lond. Math. Soc.* **12**, 73–89.

Saffman, P. G. 1992 *Vortex Dynamics*. Cambridge University Press.

Sarpkaya, T. 1975 An inviscid model of two-dimensional vortex shedding for transient and asymptotically steady separated flow over an inclined flat plate. *J. Fluid Mech.* **68**, 109–129.

Tricomi, F. 1951 *Funzioni ellittiche*. Zanichelli, Bologna.

Zannetti, L. & Franzese, P. 1994 The non-integrability of the restricted problem of two vortices in closed domains. *Physica* D **76**, 99–109.

Zannetti, L. & Iollo, A. 2003 Passive control of the vortex wake past a flat plate at incidence. *Theor. Comput. Fluid Dyn.* **16**, 211–230.

Zannetti, L., Gallizio, F. & Ottino, G. 2007 Vortex capturing vertical axis wind turbine. *J. Phys. Conf. Series* doi:10.1088/1742-6596/75/1/012029 **75**, 1–10.